Compressional velocity, seismic attenuation and permeability relationships for sandstones from WOSPP

Nicolas W. Martin and R. James Brown

ABSTRACT

Some experimental results measuring P-wave phase velocity and seismic attenuation in laboratory under dry and water-saturated conditions at ultrasonic frequencies and atmospheric pressure on sandstone samples of the Milk River Formation in the Writing-on-Stone Provincial Park (WOSPP), southern Alberta, are presented and are correlated with petrophysical data obtained from these samples as clay content, porosity and permeability. These sandstone samples present transverse anisotropy (TI) after analyzing its measured phase velocities under dry conditions along three orthogonal axis. In addition, these sandstone samples present different degree of permeability anisotropy.

The principal objective of this study is try to estimate how these petrophysical properties and permeability anisotropy affect the observed behavior of P-wave phase velocities and attenuations on sandstone samples from WOSPP. Additionally, from this analysis is expected to sight which geophysical parameter, P-wave velocity or seismic attenuation, is more important for predicting permeability and its behavior from ultrasonic seismic data.

INTRODUCTION

For most of this century, oilfield theory and practice considered that rocks exhibits isotropic wave velocities, that is, the measured velocities are no direction-dependent. But actually it is known that seismic waves travel through some rocks with different velocities in different directions due to a spatial ordering of crystals, grains, cracks, bedding planes, joints or fractures - essentially an alignment of strengths or weaknesses - on a scale smaller than the length of the seismic wave. This phenomenon is called elastic anisotropy and is represented by the anisotropic elastic stiffness tensor (Anderson *et al*., 1974; Crampin, 1978; 1981; 1984a,b; Crampin *et al*., 1984).

If there exists any elastic anisotropy caused by horizontal fine layering or fractures, it implies that, in addition to an anisotropic elastic stiffness tensor, the material will show an additional dynamic effect due to anisotropic permeability (Gelinsky and Shapiro, 1994a,b; 1995). For materials showing transverse isotropy, due to the presence of horizontal fine layering, the permeability - the ease with which fluids flow through rock - measured parallel to the layers of porous sedimentary rocks can be greater than the permeability measured vertically ($k_h > k_v$). On the other hand, for rocks that are azimuthally anisotropic due to parallel fracture planes, the permeability measured perpendicular to the fracture planes is smaller than the permeability of the rock measured parallel to the fractures ($k_h < k_v$) (Gelinsky and Shapiro, 1994a,b; 1995).

Several approaches have been used, principally at ultrasonic frequencies in laboratory, for estimating permeability anisotropy from other rock measured properties. Gibson and Toksöz (1990) predicted how the permeability would vary with direction in fractured rocks based on seismic velocity anisotropy. But, the ultrasonic experimental data of Han *et al.* (1986) and Klimentos and McCann (1990) acquired on

sandstone samples shows that the attenuation coefficient is more strongly related to clay content than velocity. Additionally, Klimentos and McCann (1990) shows a strong systematic relationship between clay content and permeability and they conclude that the attenuation is the key factor in determining permeability from seismic data.

Gelinsky and Shapiro (1994a,b; 1995) shows that the effect of the permeability anisotropy on the velocity and attenuation anisotropies varies with the range of frequency through a theoretical approach for modeling the wave propagation of qP, qSV and SH waves across a homogeneous, liquid-saturated porous medium having an isotropic poroelastic matrix and permeability anisotropy using Biot theory (Biot 1956a,b; 1962). They conclude that using this model the velocity anisotropy due to the anisotropic permeability is not significant but that the attenuation coefficient is direction-dependent at seismic frequencies. On the other hand, at higher frequencies the degree of velocity anisotropy is reduced and the attenuation coefficient is anisotropic.

These experimental and theoretical results show that is feasible to obtain valuable information about the permeability and the degree of permeability anisotropy of the reservoir from the study of the behavior of the seismic attenuation coefficient with direction.

REGIONAL GEOLOGIC FRAMEWORK

The study area is located in the Writing-on-Stone Provincial Park (WOSPP), southern Alberta, about 9 km North of the international border between Canada and the United States of America, Sections 23, 25-26, 35-36, Twp1-Rge 13-W4 and the adjacent area east of the Park, Section 31, Twp1-Rge 12-W4 (topographic sheet No. 72 E/4).

The study area is located on the western margin of the Alberta Foreland Basin, in itself a sub-basin which was part of the Western interior sea extending across the Canadian Shield during most of the Late Cretaceous (William and Stelck, 1974). The regional sedimentation patterns during this time were strongly influenced by the rising Canadian Cordillera to the West, subsiding and filling the basin as displaced or allochthonous terrains which were thrusted onto the margin of the North American craton (Price, 1973; Eisbacher *et al.*, 1974; Monger and Price, 1979; Beaumont, 1981; Cant and Stockmal, 1989).

The Milk River Formation in the study area (WOSPP) is formally subdivided into three (3) members (Tovell, 1956; Meijer-Drees and Myhr, 1981) as follows:

(1) the basal Telegraph Creek Member, consisting of interbedded buff or grey shale and sandstone in transitional contact with the underlying dark grey shale of the Colorado Group.

(2) the Virgelle Member described as a light colored, fine to medium grained sandstone, conformably overlying the Telegraph Creek Member.

(3) the upper Deadhorse Coulee Member which appears as a unit of interbedded grey-brown-purple mudstones and light brown, fine-grained sandstones, unconformably overlying the uppermost, massive-weathering Virgelle sandstone ledges.

Mhyr and Meijer-Drees (1976) and Meijer-Drees and Myhr (1981) subdivided the Virgelle Member into a lower unit, a prominent, rusty brown, well-sorted, fine to

medium grained, parallel-laminated or cross-bedded sandstone; and, an upper unit of light-grey, friable, cross-bedded sandstone, commonly containing siderite pebbles and mudstone clasts, overlying the former with an erosional contact. The sandstone samples used in this study come from the lower and upper units of the Virgelle Member of the Milk River Formation.

EXPERIMENTAL METHODOLOGY

The P-wave phase velocity and seismic attenuation measurements were made using the transmission pulse method where the P-wave signal, generated by a source-transducer at the top of the sample, is transmitted through into the sample and is registered by a receiver-transducer at the bottom of the sample. The frequency used was 1.0 MHz. Panametrics V103 piezoelectric transducers were used for both P-wave source and receiver with a diameter of 1.51 cm. The transmitted and received signals were displayed on the screen of a Nicolet oscilloscope connected, through an IBM-XT, which controls the experiment, to a Perkin-Elmer 3240 seismic processing system for storage and subsequent data processing. All the measurements were performed at atmospheric pressure.

A total of sixty sandstone samples were used for P-wave phase velocity and attenuation measurements in laboratory. These sandstone samples present an average pore diameter of 200 μm and lengths between 2.8 and 7.4 cm. Each three samples from this group represent one site and indicate three orthogonal directions of measurement: two directions (HPA and HPE), 90° apart, parallel to the layering observed on the outcrops and one vertical direction (V) perpendicular to the layering. Then, twenty sandstone samples are associated with each measurement direction. In general, these samples present a maximum degree of velocity anisotropy of 20% and a permeability anisotropy between 0.2-1.3. Here, the degree of permeability anisotropy is defined as the ratio between the measured permeability parallel to the vertical direction (HPE or HPA directions), divided by the permeability measured perpendicular to this direction (V direction). A medium presenting isotropic permeability is represented by a ratio of 1.0 using this definition.

Phase velocity estimation

Dellinger (1992) showed that for propagation down symmetry directions group and phase velocity are the same and there is no ambiguity for rock samples but in nonsymmetry directions there is no guarantee the energy radiated from the source will travel straight up the axis of the sample to the receiver. Vestrum (1994) reached a similar conclusion working on Phenolic CE which was assumed to have orthorhombic symmetry. In all the experiments performed on the sandstone samples of WOSPP for estimating P-wave velocity was assumed that the measured velocities represent the P-wave phase velocities because each sample was oriented at two directions (HPA and HPE), 90° apart, parallel to the layering and one vertical direction (V) perpendicular to the layering. Additionally, the measured P-wave phase velocities along these three orthogonal axis reveals a TI symmetry which indicates that these orientation axis are very close to the symmetry axis of these sandstones. The P-wave velocity and attenuation values were very similar between HPA and HPE directions.

Rathore *et al*. (1994) proposed the first-zero-crossover method for estimating the P-wave phase velocity for a dispersive and anisotropic medium (Figure 1b). The P-wave phase velocity obtained using the traditional first-break method (Figure 1a) is related to the high-frequency components of the signal which can be significantly different from

the dominant lower-frequency phase velocity for a dispersive and anisotropic medium (Rathore *et al.* ,1993). For a dispersive medium with frequency-dependent attenuation, in which the high frequencies are lost, the dominant frequency of the received signal is relatively low and the calculated P-wave phase velocity using the first-zero-crossover method will yield a low-frequency P-wave phase velocity (Rathore *et al.*, 1994).

Then, the P-wave phase velocities for the sandstone samples from WOSPP were calculated as follows:

$$V_P = \frac{x}{t_{c,r} - t_{c,t}} \tag{1}$$

where x is the length of the sandstone sample, $t_{c,r}$ is the picked crossover traveltime of the received signal and $t_{c,t}$ is the picked crossover traveltime of the transmitted signal.

Seismic attenuation estimation

For estimating the attenuation coefficient of the sandstone samples of WOSPP was used the spectral ratio technique (Toksöz *et al.*, 1979). This method consists in comparing the spectral amplitudes between a reference sample and a sandstone sample at different frequencies. Because attenuation implies a preferential loss of the high frequencies, a change in the total spectrum will therefore occur.

Using this spectral ratio technique is possible to remove experimental variables which affect the measured attenuation as the effects on the absolute amplitudes by the measurement system and the frequency response of the transducers considering that experimental conditions (geometry, coupling conditions, transducers) remain unchanged during the experiment (Toksöz *et al.*, 1979).

The amplitudes for a reference sample and a sandstone sample are related in the spectral ratio method as:

$$\ln(A_1/A_2) = \ln(G_1/G_2) + (\alpha_2 - \alpha_1)x \tag{2}$$

where A_1 and A_2 are the amplitudes for reference and sandstone samples, respectively, G_1, G_2 and α_1, α_2 are its corresponding geometrical factors and attenuation coefficients and x is the sample's length. By assuming $\alpha(f)$ is a linear function of the frequency (Toksöz *et al.*, 1979):

$$\alpha(f) = \gamma f \tag{3}$$

and keeping the same geometry for both the reference and sandstone samples, then G_1/G_2 is a frequency-independent scale factor and eq. (2) is reduced to:

$$\ln(A_1/A_2) = \ln(G_1/G_2) + (\gamma_2 - \gamma_1)xf \tag{4}$$

If the spectral ratio $\ln(A_1/A_2)$ is plotted against frequency f, then $(\gamma_2 - \gamma_1)$ can be found from the slope by least-squares linear regression. In the laboratory is normally used aluminum as reference sample because it has a neglective attenuation coefficient. As a result, the attenuation coefficient of the sandstone sample can be determined directly from the slope of the above linear relation.

Diffraction corrections

Seki *et al*. (1956) and Papadakis (1966) established that during performing experiments in laboratory for estimating velocity and attenuation measurements using piezoelectric transducers for generating and receiving ultrasonic waves, is important to correct properly the diffraction effect due to the finite-size of the transducers because the diffraction effects adds to the attenuation appreciably, hidden its real value, while raising the velocity lightly.. Papadakis (1966) calculated the phase ϕ and attenuation in dB as a function of a normalized distance S_c, defined as:

$$S_c = \frac{z\nu}{r^2 f_c} \tag{5}$$

where z is the propagation distance, ν is the phase velocity, r is the transducer radius and f_c is the central frequency of the broad-band pulse. Additionally, Papadakis (1966) showed that the velocity correction due to the finite-size of the transducers is given as function of an increment in traveltime, Δt by the following expression:

$$t = t' + \Delta t \tag{6}$$

where the increment Δt is to be added to the measured value t' of the first arrival or first zero-crossing traveltimes to get the true traveltime t. Then, the phase velocity after applying the diffraction correction is lower than obtained without considering this correction because the traveltime is increased keeping the length of the sample constant.

On the other hand, the attenuation correction $\Delta\alpha$ is subtracted from the measured attenuation α' to get the true attenuation α as follows:

$$\alpha = \alpha' - \Delta\alpha \tag{7}$$

The obtained P-wave phase velocity and attenuation measurements on the sandstone samples were corrected for diffraction and edge effects as result of the finite-size of the transducers using the tabulated corrections published by Benson and Kiyohara (1974) based on the analyses of Papadakis (1966). These corrections Δt and $\Delta\alpha$ are expressed as function of the normalized distance S_c.

ANALYSIS OF RESULTS

Permeability-porosity relationship

Figure 1 shows the permeability-porosity relationship observed on the sandstone samples from WOSPP. Because the sandstones from the lower and upper units of the Milk River Formation present different geophysical and petrophysical behaviors, these sandstones will be called LU and UU sandstones, respectively. It is evident that exist two different trends: for LU sandstones the permeability-porosity relationship is linear on a semilog plot as expected from statistical analysis of well log information (Allen, 1979; Wendt *et al*., 1986); in contrast, for UU sandstones the permeability is practically independent on porosity indicating that porosity no controls the measured permeability values for these sandstone samples. A linear least-squares fit was applied on the permeability-porosity values for LU sandstones giving a correlation factor of 0.83 (Figure 1). For LU sandstones is believed that the geometry of the pores is controlling the permeability.

Permeability-clay content relationship

Figure 2 shows the measured permeability-clay content relationship for LU and UU sandstones. For LU sandstones clay content strongly affects its corresponding permeability values indicating that permeability tends to increase for clay content between 7-10 %, but it decreases (around of 400 mD) when clay content increases over 10 %. Additionally, it is concluded that clay content and porosity are the principal factors controlling the measured permeability-porosity relationship for these sandstones. For UU sandstones, clay content also affects its permeability values where high permeability values are associated with high clay content values. As conclusion, the permeability-clay content relationship is the most important for UU sandstones.

Porosity-clay content relationship

The experimental porosity-clay content relationship is shown in Figure 3. It is observed that porosity increases very gently with increasing clay content. Then, clay content appears as a secondary factor affecting the original porosity of these sandstone samples.

Effect of the saturant fluid on P-wave velocity anisotropy

Figure 4a shows the relationship between the vertical and horizontal (HPA) P-wave phase velocities under dry conditions at atmospheric pressure at 1.0 MHz. It is observed from this graph that both velocities follow a linear trend showing a TI behavior. In fact, this linear trend is above the solid line which represents the isotropic velocity pattern indicating that the horizontal (HPA) P-wave velocity values are higher than the corresponding vertical P-wave velocity values. The same behavior was observed for the measured P-wave velocity along the other horizontal (HPE) direction.

The effect of the saturant fluid on the above velocity anisotropy is indicated in Figure 4b. It is evident that the presence of fluid into the pore of the sandstone samples produces that the observed velocity anisotropy under dry conditions is diminished and the P-wave velocities under saturated conditions are more isotropic. Although some samples show a stronger velocity anisotropy under water-saturated conditions, in general the P-wave velocity values are very close to the line which defines the velocity isotropy condition.

P-wave velocity, clay content, porosity and permeability relationships

Figure 5a shows the effect of the permeability on the P-wave velocity for LU and UU sandstones under water-saturated conditions having similar clay content and porosity values. The porosity range for LU sandstones is between 27.8 and 29.4 % and between 29.0 and 31.0 % for UU sandstones. It is evident that the P-wave phase velocity associated with LU and UU not shows a significant variation with permeability (Akbar *et al*., 1993; Klimentos and McCann, 1990; Klimentos, 1991). Figure 5b shows the variation of the compressional velocity as function of permeability for LU sandstones with clay content of 6.5 % but considering porosity variation between 20-26 %. The principal effect of the porosity is to reduce the P-wave velocity. Additionally, the P-wave velocity for both LU and UU sandstones is affected by clay content producing a velocity decrement with increasing clay content (Figure 5c). It indicates that the principal factors that affect the P-wave velocity are clay content and porosity (Klimentos, 1991).

The P-wave velocity-porosity relationships observed on LU sandstones for both vertical and horizontal (HPA) directions are indicated in Figures 6a,b, respectively. The lineal trend indicating that the P-wave velocity decreases with increasing porosity is observed on both directions. Also, the P-wave velocity is no direction-dependent because the porosity values are very similar along both directions. For UU sandstones any clear trend between compressional velocity and porosity was observed along three directions. Figure 6c shows the P-wave velocity behavior along vertical direction.

Figures 7a,b show the permeability anisotropy effect on the measured P-wave velocities under water-saturated conditions. The HPA direction shows higher permeability values than measured along vertical direction The permeability anisotropy effect is no significant because any velocity pattern change is observed for both vertical and horizontal (HPA) directions. Again, it is evident that the P-wave velocity-permeability relationship is no significant for UU sandstones and the effect of permeability on P-wave velocity for LU sandstones is principally a porosity and clay content effect as indicated before.

Attenuation coefficient, porosity and permeability relationships

The experimental attenuation-permeability relationship with constant clay content for LU and UU sandstones is indicated in Figure 8. The porosity range for LU sandstones is between 27.8 and 29.4 % and between 29.0 and 31.0 % for UU sandstones. Unlike P-wave velocity, the attenuation for P waves is strongly affected by the permeability which is controlled principally by clay content. For both LU and UU sandstones the P-wave attenuation coefficient increases with increasing permeability.

The effect of porosity on P-wave attenuation coefficient is shown in Figure 9. It is evident that attenuation coefficient tends to increase with increasing porosity. This effect is similar to permeability effect on attenuation (Figure 8) making very difficult to isolate the effect of each one on attenuation with the present data. Additionally, for P-wave attenuation coefficient is not possible distinguish between LU and UU sandstones because both present very similar values of this property.

Figures 10a,b show that the permeability anisotropy for these sandstones not produces significant attenuation variation but along both vertical and HPA directions the attenuation coefficient tends to increase with increasing the permeability indicating that this property could be more suitable to be used for estimating permeability behavior from seismic data. But all the experimental relationships presented in this study are

valid at ultrasonic frequencies and its application at seismic frequencies is always a controversial discussion.

Effect of saturant fluid on attenuation coefficient

The effect of the saturant fluid on the attenuation oefficient is shown in Figure 11b. Under dry conditions the attenuation coefficient values are close to the line which defines that the measured attenuation along the vertical direction is equal to the measured attenuation along HPA direction (Figure 11a). In contrast, the attenuation coefficient shows a more anisotropic behavior under water-saturated conditions as represented by the high scatering of the attenuation coefficient values (Figure 11b)

ACKNOWLEDGMENTS

We would like to acknowledge Rodolfo Meyer for donating the sandstone samples used in this study. His important participation and enlightened discussions are also appreciated. We wish to thank the sponsors of the CREWES Project at the University of Calgary for their support of this study. We wish to thank the staff of the CREWES Project and Core Laboratories in Calgary for enabling us to continue this work.

A personal recognition is given by Nicolas Martin to Maria Donati and her mother for their faith and moral support during the development of this study. Also, we wish to thank Lagoven, S. A. in Venezuela for all its support.

REFERENCES

Akbar, N., Dvorkin, J. and Nur, A., 1993, Relating P-wave attenuation to permeability: Geophysics, v. 58, p. 20-29.

Anderson, D. L., Minster, B. and Cole, N., 1974, The effect of oriented cracks on seismic velocities: J. Geophys. Res., v. 79, p. 4011-4015.

Beaumont, C., 1981, Foreland basins: Geophys. J. R. Astr. Soc., v. 55, p. 291-329.

Biot, M. A., 1956a, Theory of propagation of elastic waves in a fluid-saturated solid. I, Lower frequency range: J. Acoust. Soc. Am., v. 28, p. 168-178.

— , 1956b, Theory of propagation of elastic waves in a fluid-saturated solid. II, Higher frequency range: J. Acoust. Soc. Am., v. 28, p. 179-191.

— , 1962, Mechanics of deformation and acoustic propagation in porous media: J. Appl. Phys., v. 23, p. 1482-1498.

Cant, D. J. and Stockmal, G. S., 1989, The Alberta foreland basin: relationship between stratigraphy and Cordilleran terrane-accretion events: Canadian Journal of Earth Sciences, v. 26, p. 1964-1975.

Crampin, S., 1978, Seismic-wave propagation through a cracked solid: Polarization as a possible dilatancy diagnostic: Geophys. J. R. Astr. Soc., v. 53, p. 467-496.

— , 1981, A review of wave motion in anisotropic and cracked elastic-media: Wave Motion, v. 3, p. 343-391.

— , 1984a, Anisotropy in exploration geophysics: FIRST BREAK, v. 2, No. 3, p. 19-21.

— , 1984b, An introduction to wave propagation in anisotropic media: Geophys. J. R. Astr. Soc., v. 76, p. 17-28.

Dellinger, J. and Vernik, L., 1994, Do traveltimes in pulse-transmission experiments yield anisotropic group or phase velocities?: Geophysics, v. 59, p. 1774-1779.

Eisbacher, G. H., Carrigy, M. A. and Campbell, R. B., 1974, Paleodrainage patterns and late orogenic basins of the Canadian Cordillera. *In* Dickinson, W. R. (Ed.): Tectonics and sedimentation. Society of Economic Paleontologists and Mineralogists, Special Publication, v. 22, p. 143-166.

Gelinsky, S. and Shapiro, S. A., 1994a, Poroelastic velocity and attenuation in media with anisotropic permeability: 64th Ann. Internat. Mtg., Soc. Expl. Geophys., Expanded Abstracts, p. 818-821.

— , 1995, Anisotropic permeability: influence on seismic velocity and attenuation: accepted for publication in: Proceedings of the 6IWSA, (Trondheim, Norway).

Gibson, R. L. Jr. and Toksöz, M. N., 1990, Permeability estimation from velocity anisotropy in fracture rocks: J. Geophys. Res., v. 95, p. 15643-15655.

Klimentos, T. and McCann, C., 1990, Relationships between compressional wave attenuation, porosity, clay content, and permeability of sandstone: Geophysics, v. 55, p. 998-1014.

Klimentos, T., 1991, The effects of porosity-permeability-clay content on the velocity of compressional waves: Geophysiscs, v. 56, p. 1930-1939.

Meijer-Drees, N. C. and Mhyr, D. W., 1981, The Upper Cretaceous Milk River and Lea Park Formations in southeastern Alberta: Bull. Can. Petroleum Geology, v. 29, No. 1, p. 42-74.

Mhyr, D. W. and Meijer-Drees, N. C., 1976, Geology of the southeastern Alberta Milk River Gas Pool. *In*: The sedimentology of selected elastic oil and gas reservoirs in Alberta. Canadian Society of Petroleum Geologists, Calgary, Alberta.

Monger, J. W. H. and Price, R. A., 1979, The geodynamic evolution of the Canadian Cordillera - progress and problems: Canadian Journal of Earth Sciences, v. 16, p. 770-791.

Papadakis, E. P., 1976, Ultrasonic diffraction from single apertures with applications to pulse measurements and crystal physics. Physical Acoustics XI, p. 151-211. Academic Press Inc.

Price, R. A., 1973, Large-scale gravitational flow of supracrustal rocks, southern Canadian Rocky Mountains. *In* De Jong, K. A. and Scholten, R. A. (Eds.): Gravity and Tectonics, Wiley Interscience, New York, p. 491-502.

Rathore, J. S., Fjaer, E., Renlie, L. and Nysaeter, J., 1993, Estimation of phase velocities in cracked rocks: 55th EAEG meeting, Stavanger, Norway, Expanded Abstracts, p. 124.

Rathore, J. S., Fjaer, E., Holt, R. M. and Renlie, L., 1994, P- and S-wave anisotropy of a synthetic sandstone with controlled crack geometry: Geophys. Prosp., v. 43, p. 711-728.

Seki, H., Granato, A. and Truell, R., 1956, Diffraction effects in the ultrasonic field of a piston source and their importance in the accurate measurement of attenuation: J. Acoust. Soc. Am., v. 28, p. 230-238.

Toksöz, M. N., Johnston, D. H. and Timur, A., 1979, Attenuation of seismic waves in dry and saturated rocks: I. Laboratory measurements: Geophysics, v. 44, p. 681-690.

Tovell, W. M., 1956, Some aspects of the geology of the Milk River and Pakowki Formations (southern Alberta): University of Toronto, Ph-D Thesis, 129p.

Vestrum, R. W., 1994, Group- and phase-velocity inversion for the generl anisotropic stiffness tensor: M. Sc. Thesis, Univ. of Calgary.

Williams, G. D. and Stelck, C. R., 1975, Speculations on the Cretaceous palaeogeography of North America. *In* Caldwell, W. G. E. (Ed.): The Cretaceous System in the western interior of North America: The Geological Association of Canada, Paper No. 13, p. 1-20.

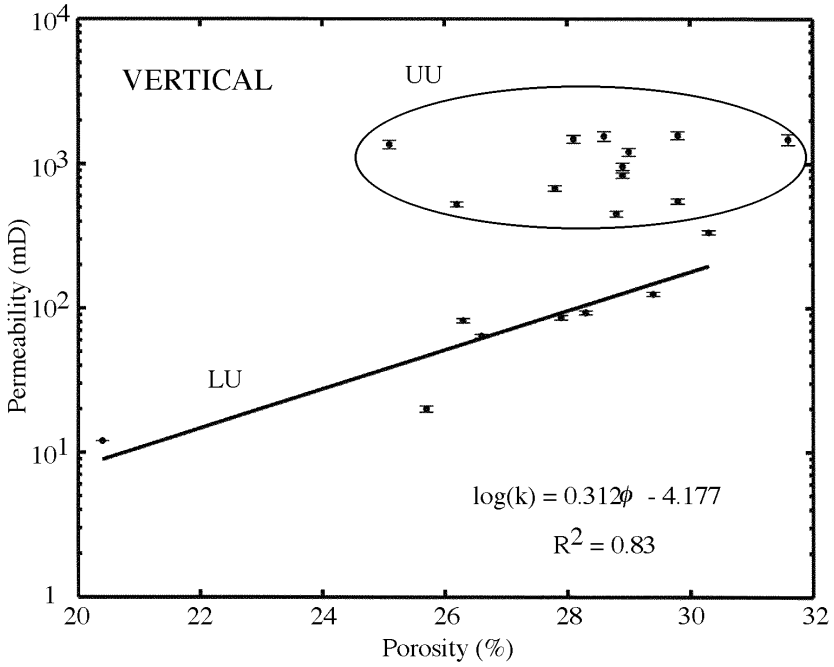

Figure 1 Experimental permeability-porosity relationship for LU and UU sandstones.

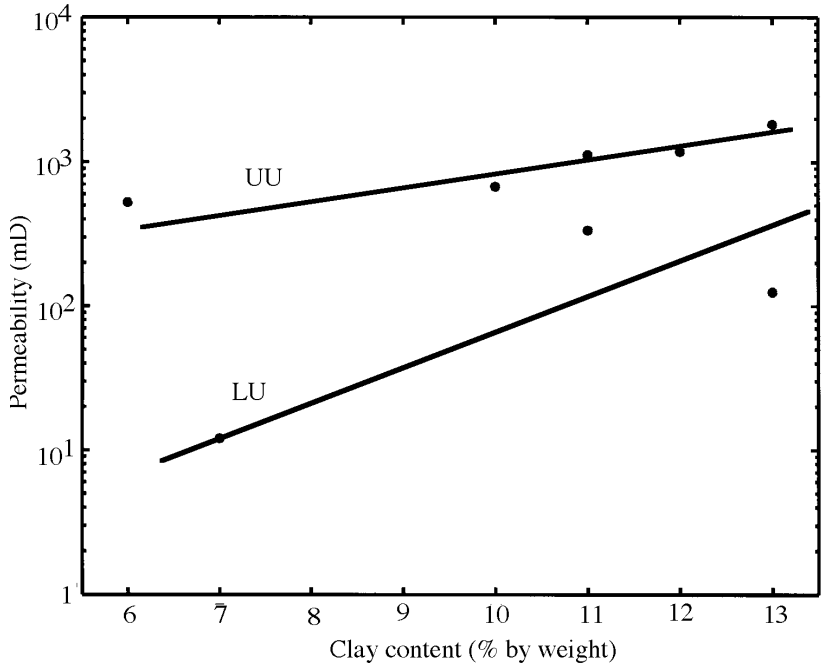

Figure 2 Effect of clay content on permeability for LU and UU sandstones.

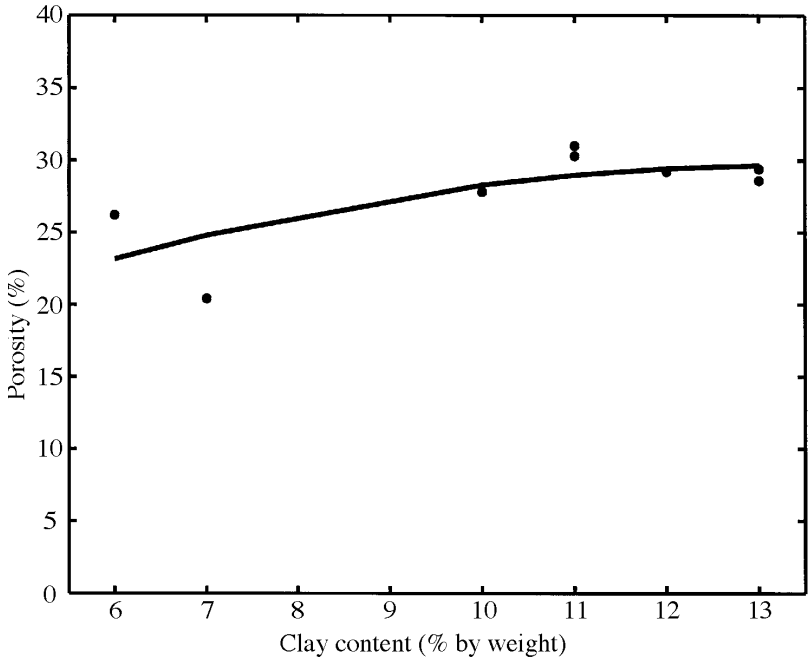

Figure 3 Porosity-clay content relationship observed on the sandstone samples from WOSPP.

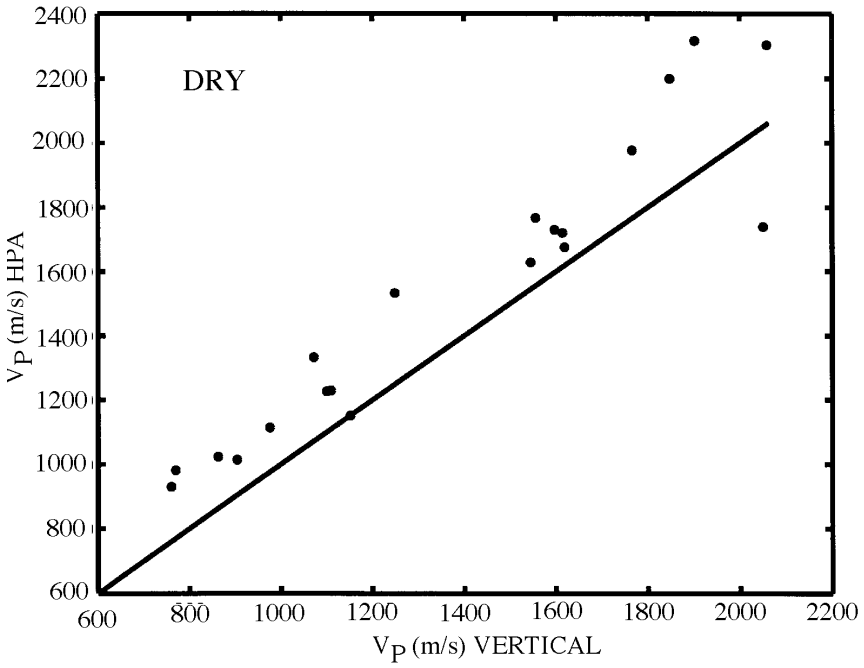

(a)

Figure 4 (a) Relation between the measured P-wave velocities along vertical and horizontal (HPA) directions under dry condition. The line indicates the case when both velocities are equal (ivelocity isotropy).

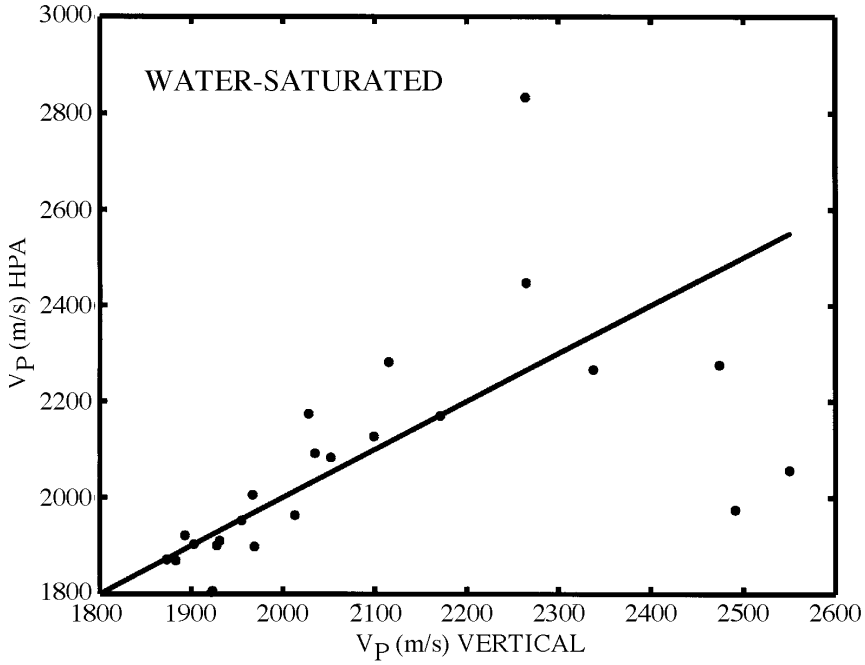

(b)

Figure 4 (b) Relation between the measured P-wave velocities along vertical and horizontal (HPA) directions under water-saturated condition. The line indicates the case when both velocities are equal (ivelocity isotropy).

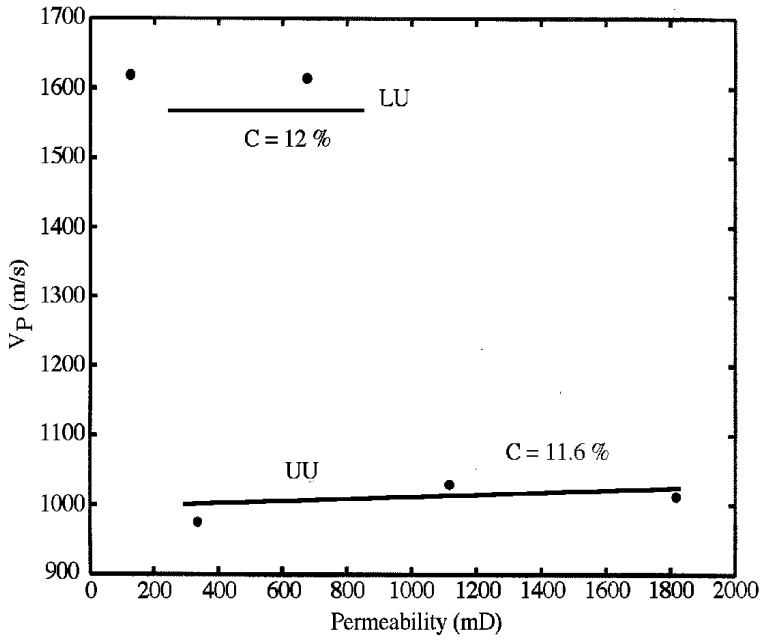

(a)

Figure 5 (a) P-wave velocity-permeability relationships for LU and UU sandstones. Clay content and porosity keep constant.

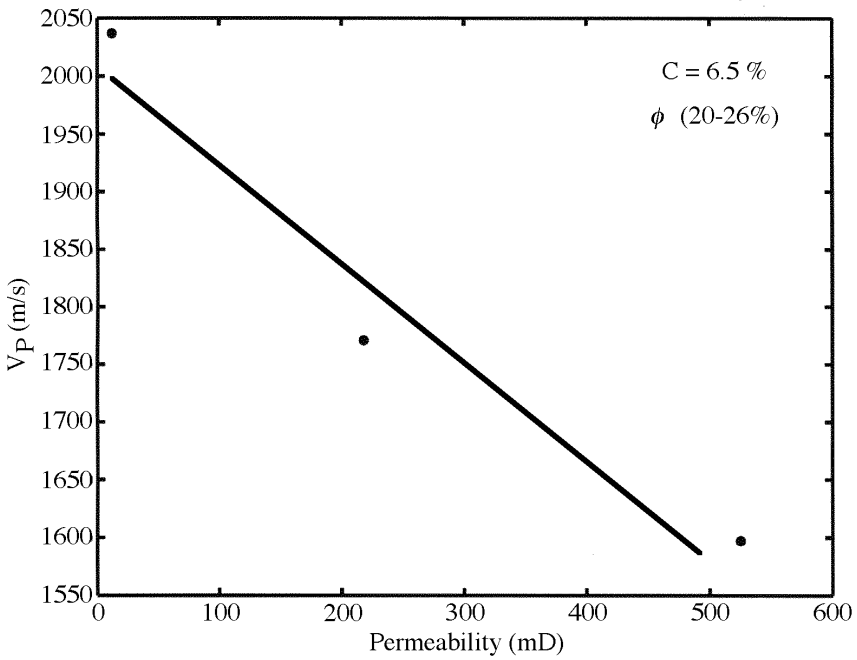

(b)

Figure 5 (b) P-wave velocity-permeability relationship for LU and UU sandstones. Clay content fixed but variable porosity. The porosity values are between 20 and 26 %.

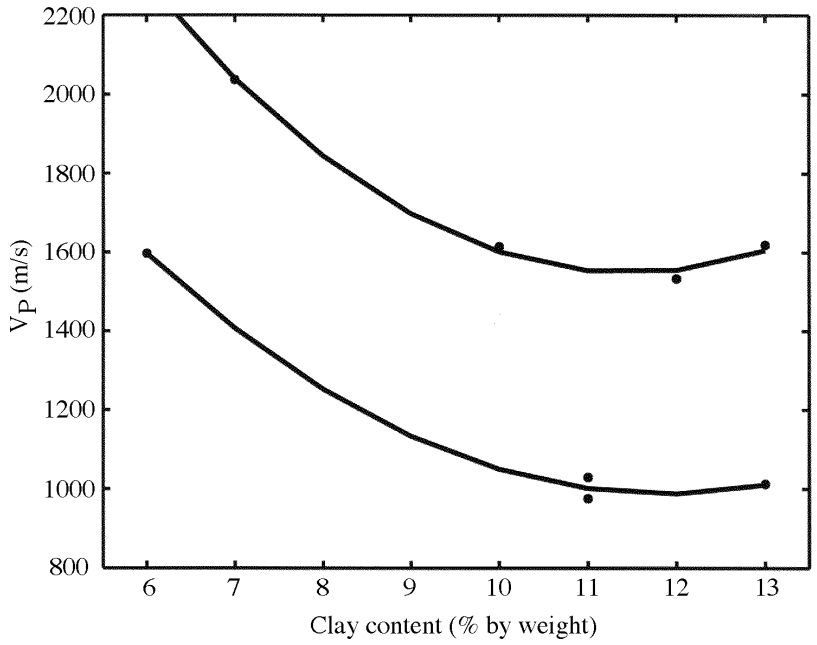

(c)

Figure 5 (c) P-wave velocity-clay content relationship. The upper curve represent this relation for LU sandstones with porosities between 20.4 and 30 %. The lower curve is the corresponding relationship for UU sandstones with porosities between 26.2 and 31 %.

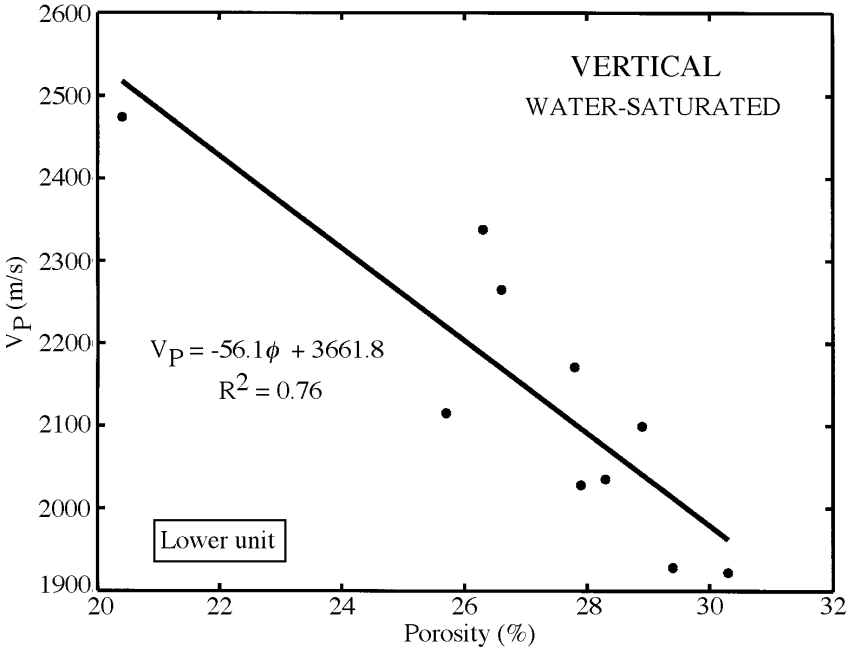

(a)

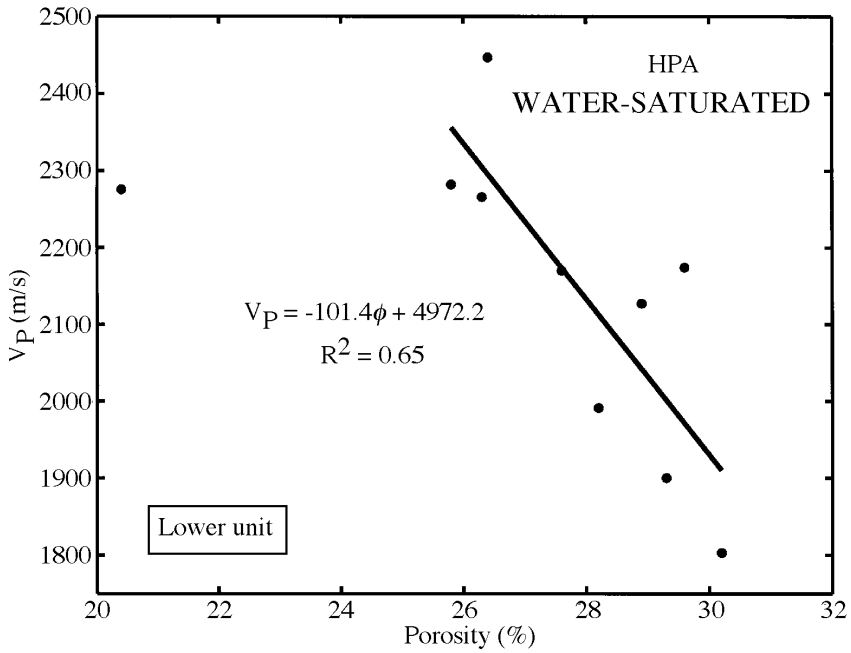

(b)

Figure 6 Variation of the P-wave velocity as function of the porosity under water-saturated condition for LU sandstones. (a) measured along vertical direction. (b) measured along the horizontal (HPA) direction

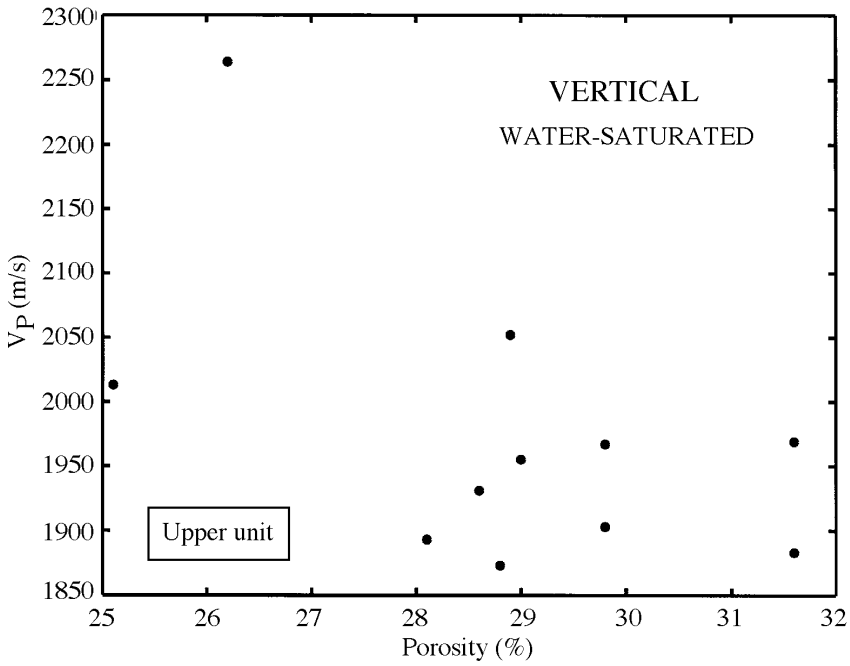

(c)

Figure 6 (c) Variation of the P-wave velocity as function of the porosity under water-saturated condition measured along vertical direction for UU sandstones.

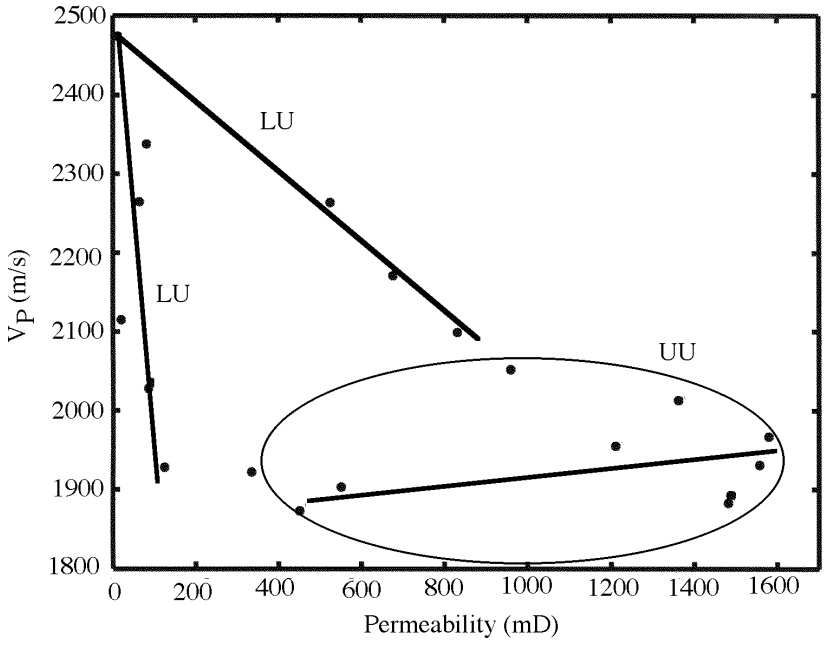

(a)

Figure 7 (a) P-wave velocity-permeability relationship under water-saturated condiion for LU and UU sandstones measured along vertical direction.This graph shows a linear trend for LU sandstones but no significant relation between P-wave velocity and permeability for UU sandstones

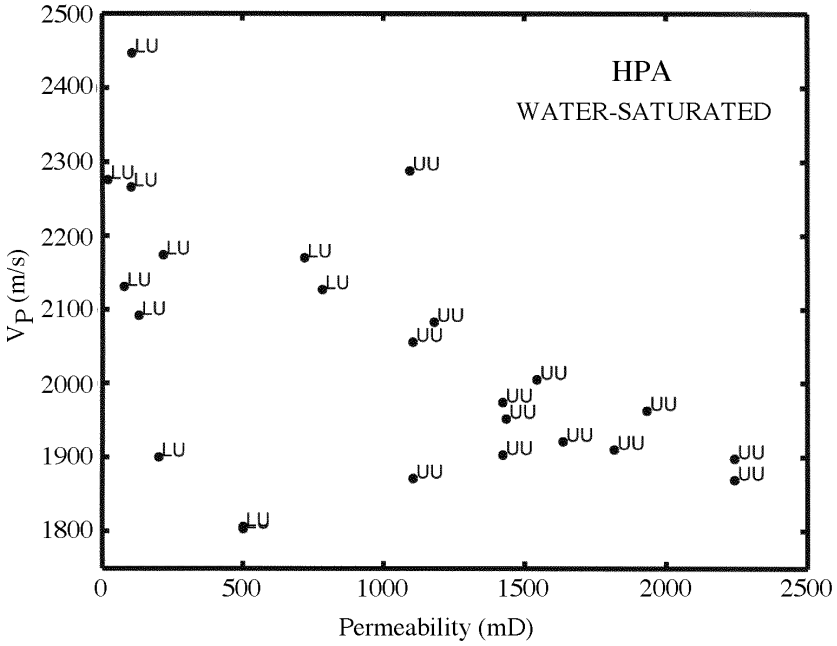

(b)

Figure 7 (b) P-wave velocity-permeability relationship under water-saturated condiion for LU and UU sandstones measured along the horizontal (HPA) direction.

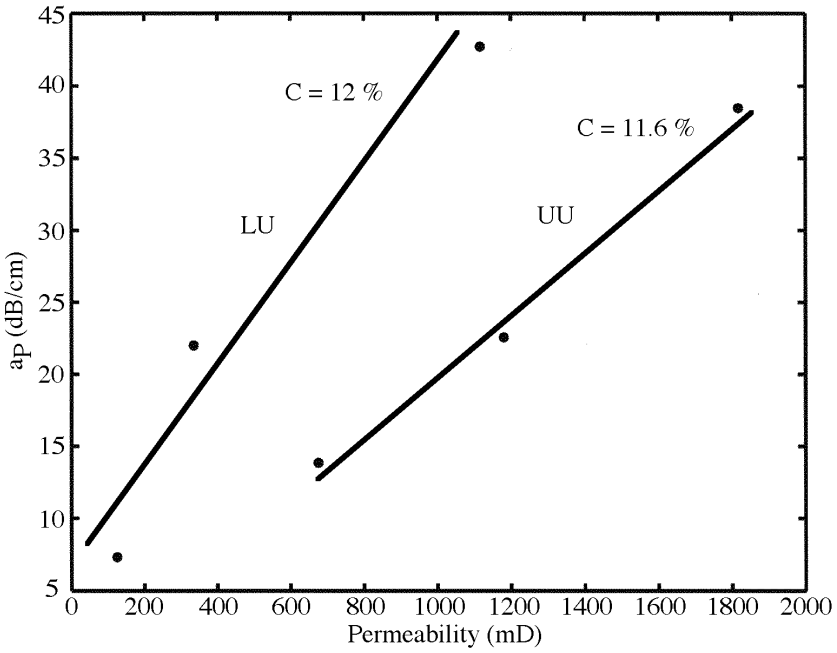

Figure 8 Experimental attenuation-permeability relationship for LU and UU sandstones keeping clay content constant at 12 %.

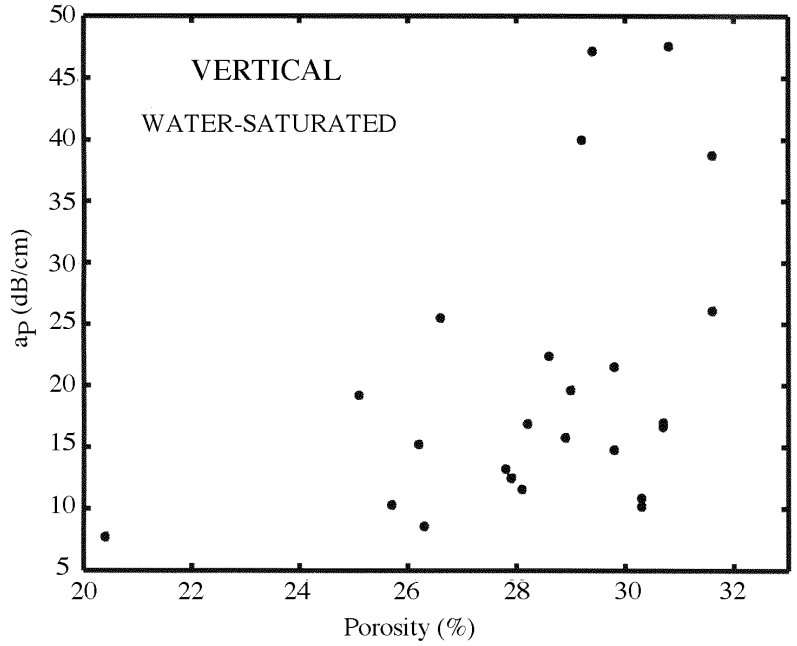

Figure 9 Graph showing the observed relationship between attenuation coefficient and porosity along the vertical direction under saturated conditions for LU and UU sandstones.

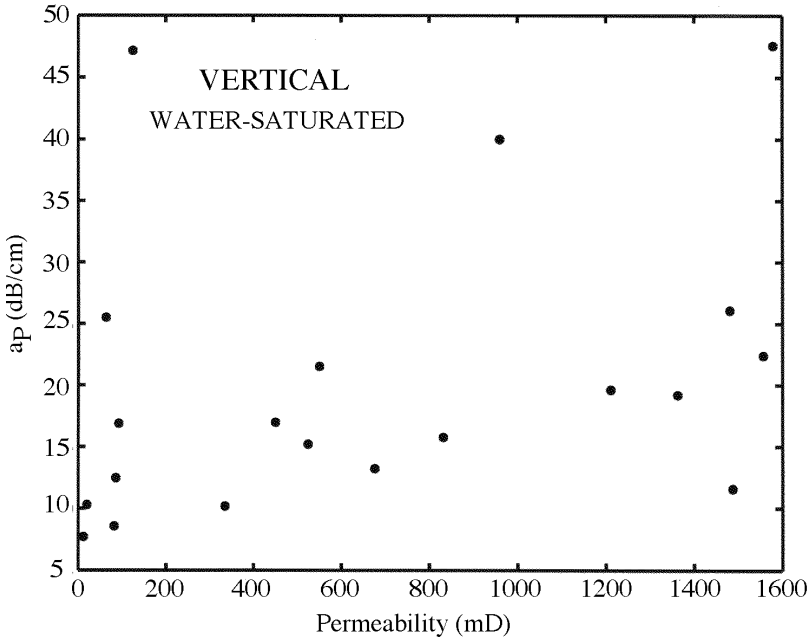

(a)

Figure 10 (a) Experimental P-wave attenuation-permeability relationship measured along the vertical direction.

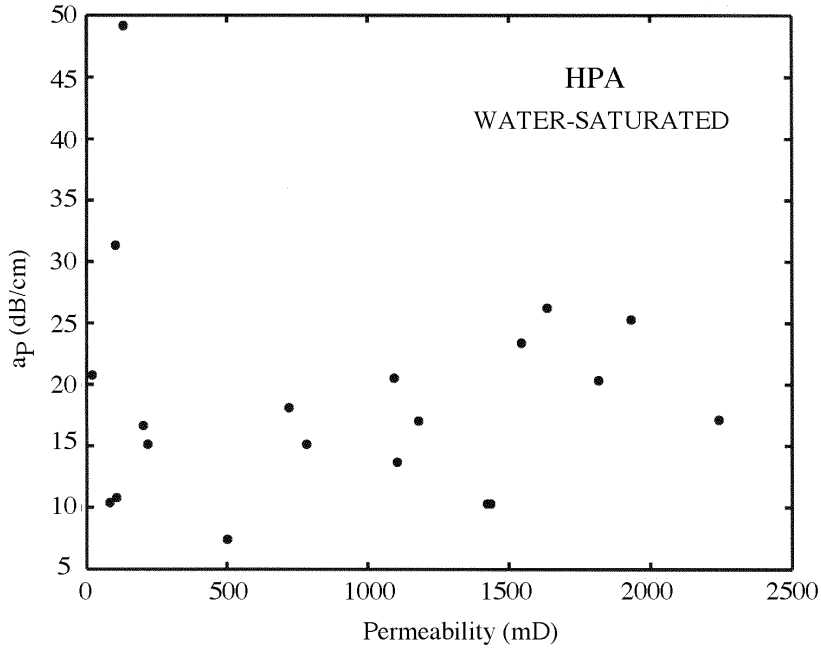

(b)

Figure 10 (b) Experimental P-wave attenuation-permeability relationship measured along horizontal (HPA) direction.

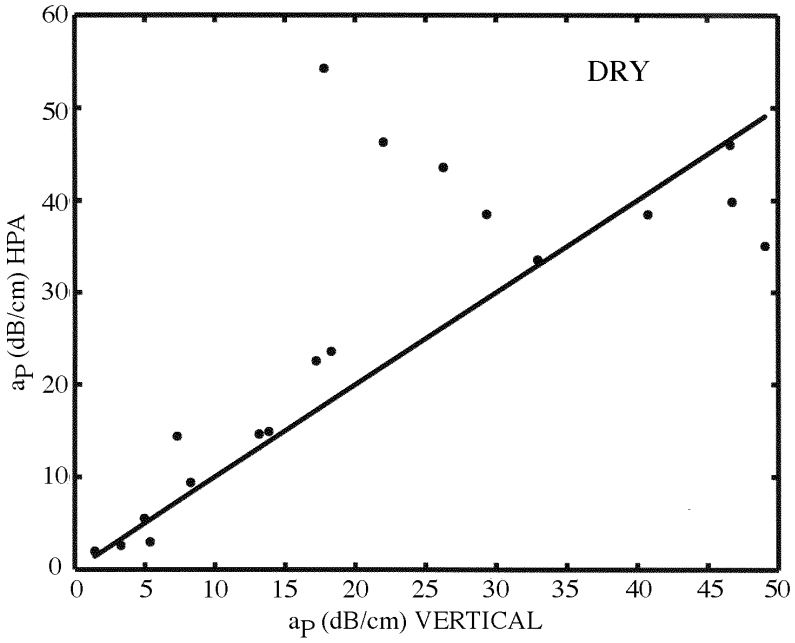

(a)

Figure 11 (a) P-wave attenuation coefficient anisotropy for LU and UU sandstones under dry condition. The bold line represents that both vertically and horizontally measured attenuations are equal. The horizontal direction is HPA axis.

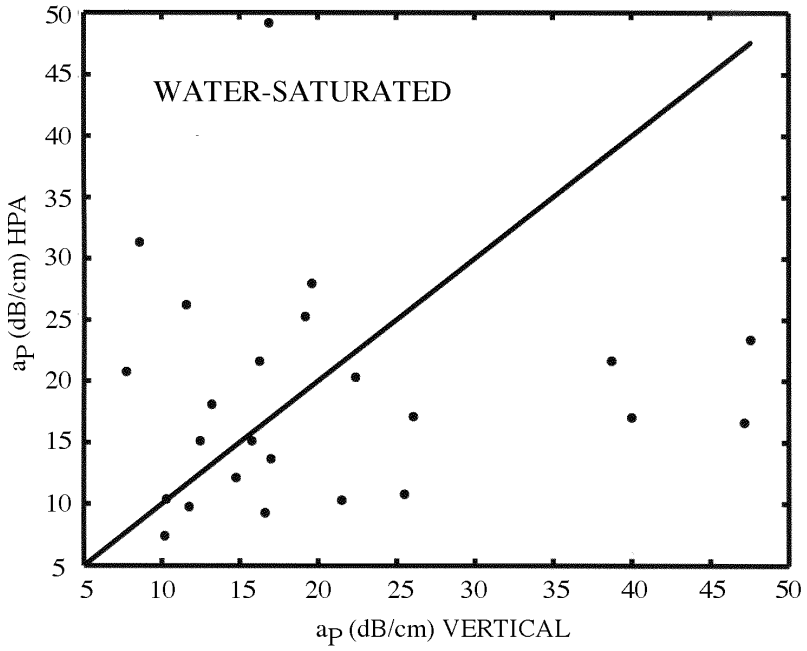

(b)

Figure 11 (b) P-wave attenuation coefficient anisotropy for LU and UU sandstones under water-saturated conditions. The bold line represents that both vertically and horizontally measured attenuations are equal. The horizontal direction is HPA axis.